Biochemical and Biophysical Research Communications 395 (2010) 70–75

Contents lists available at ScienceDirect

Biochemical and Biophysical Research Communications

journal homepage: www.elsevier.com/locate/ybbrc

Vibrio harveyi hemolysin induces ultrastructural changes and apoptosis in flounder (*Paralichthys olivaceus*) cells

Fangfang Bai [a], Boguang Sun [a], Norman Y.S. Woo [b], Xiao-Hua Zhang [a,*]

[a] Department of Marine Biology, Ocean University of China, 5 Yushan Road, Qingdao, China
[b] Biology Department, Chinese University of Hong Kong, Hong Kong

ARTICLE INFO

Article history:
Received 11 January 2010
Available online 27 March 2010

Keywords:
Vibrio harveyi hemolysin
Erythrocytes
Flounder cell line
Ultrastructure changes
Apoptosis

ABSTRACT

Vibrio harveyi hemolysin (VHH) is considered a major pathogenic virulence factor to fish. However, the VHH active-site mutant has lost all hemolytic and phospholipase activities as well as pathogenicity. In this study, the effect of VHH on erythrocytes and a gill cell line from flounder was elucidated. Erythrocyte membranes formed thin tubular protrusions immediately after exposure to VHH, and membrane corrugations were evident after extended incubation. In contrast, the mutant VHH did not induce any gross morphological changes. With VHH-treated FG-9307 cells, a cell line derived from flounder gill, destruction of organelles and formation of features resembling apoptotic bodies were observed. Immunogold staining showed that a large amount of VHH was deposited on the membranes and membrane debris of erythrocytes and FG-9307 cells after treatment with VHH. Apoptotic features, such as chromatin condensation and apoptotic bodies, were observed in VHH-treated FG-9307 cells using DAPI staining. Moreover, cell cycle analysis showed that VHH increased the proportion of cells in G1 phase. In addition, VHH significantly increased the percentage of apoptosis, the number of TUNEL positive apoptotic cells, and caspase-3 activity in FG-9307 cells when compared with the untreated controls. These data suggested that VHH killed the cells through apoptosis via the caspase activation pathway.

1. Introduction

Vibrio harveyi is an important bacterial pathogen to cultured penaeid shrimp and fish [1], and it can also cause infections in humans [2]. Although the pathogenic mechanisms of this organism are not well understood, hemolysin has been considered to be a major virulence factor [3,4].

Hemolysin is one of the most widely distributed exotoxins among pathogenic vibrios, and exerts various roles in the infective process [5]. The mechanism of action of hemolysin involves acting as either a pore-forming protein or a phospholipase [6], and some hemolysins have both of these activities [7]. The pore-forming hemolysins are normally secreted in a soluble form and exert their catalytic effect by assembling into a transmembrane pore, such as the TDH of *V. parahaemolyticus* [8]. However, the action mechanism of the hemolysins involving phospholipase activity has not been clearly defined. Phospholipase has the ability to hydrolyze phospholipids and generate reaction products which may either lead to the loss of membrane integrity and cytotoxicity [9,10] or act as second messengers (such as fatty acids or lysophosphatidylcholine) to elicit or suppress inflammation or apoptosis [11,12].

Previously, we cloned two closely related VHH hemolysin genes from a highly pathogenic *V. harveyi* isolate [13], which were very similar to the *tlh* gene of *V. parahaemolyticus* [14]. Furthermore, we obtained purified recombinant VHH protein, and found that VHH is a monomer protein with a molecular mass of ~44.3 kDa, composed of 398 amino acids. The VHH was demonstrated to be either a lysophospholipase or phospholipase B [15]. VHH was cytotoxic against flounder gill cells (FG-9307) in tissue culture, and had strong pathogenicity to flounder when injected intraperitoneally [4]. We also obtained a null-mutant protein of VHH via site-directed mutagenesis, in which the center residue, Ser153, of the active-site in the catalytic reaction of VHH, was replaced by a glycine, a neutral residue. The mutant VHH resulted in the complete loss of hemolytic, phospholipase and pathogenic activity of VHH [15].

In this study, we investigated the action mode of VHH on flounder erythrocytes, and compared with that of the VHH null-mutant protein. Additionally, the ultrastructural changes induced by VHH in flounder gill cells (FG-9307) were studied to elucidate its cytotoxic mechanism. Finally, to address if the toxicity exerted by VHH in host cell were partly due to apoptosis, we performed DAPI staining, TUNEL assay, cell cycle analysis and caspase activity assay. These studies constitute an effort to demonstrate the attack mechanism of VHH to eukaryotic cells.

Abbreviations: VHH, *Vibrio harveyi* hemolysin; TDH, thermostable direct hemolysin; TUNEL, terminal deoxynucleotidyl transferase-mediated dUTP nick end labeling; DAPI, 4′-6-diamidino-2-phenylindole.

* Corresponding author. Fax: +86 532 82032767.
E-mail address: xhzhang@ouc.edu.cn (X.-H. Zhang).

0006-291X/$ - see front matter © 2010 Elsevier Inc. All rights reserved.
doi:10.1016/j.bbrc.2010.03.141

2. Materials and methods

2.1. Preparation of VHH and mutant VHH

Purification and hemolytic units (HU) determination of VHH and mutant VHH were performed according to the procedure previously described [4,15].

2.2. Isolation of erythrocytes

Flounder blood was drawn with heparinized syringe, and erythrocytes were isolated from 10 ml of fresh blood by centrifugation at 1500 *g* for 10 min at 4 °C. The pelleted erythrocytes were washed three times in TBS buffer (20 mM Tris in 0.9% NaCl, pH 7.2).

2.3. FG-9307 cell culture

The continuous cell line, FG-9307, has been previously established from gills of flounder, *Paralichthys olivaceus* [16]. The cells were cultured at 20 °C in Minimal Essential Medium (MEM, Gibco, USA), supplemented with 10% bovine calf serum (BCS, Gibco), 100 μg/ml penicillin and 100 μg/ml streptomycin. According to previous study [4], the IC_{50} value of VHH to FG-9307 cells was 2.5 μg/ml and this concentration was therefore used to incubate with FG-9307 cells in this study.

2.4. Scanning electron microscopy (SEM)

Erythrocytes were incubated with purified VHH (16 HU) and mutant VHH (the same protein concentration as for VHH) for 0.5, 5, 10, 20, 45 min and 2 h, and prepared for subsequent examination by SEM. Following incubation, the samples were fixed with 2.5% (v/v) glutaraldehyde in phosphate-buffered saline (PBS, pH 7.4) for 4 h and immediately spread onto 1% alcian blue-treated coverglasses for 20 min. The samples were then fixed first with 2.5% glutaraldehyde for 30 min, followed by 1% osmium tetroxide for 1 h. Specimens were dehydrated in a graded ethanol series (30–100%), critical-point dried in carbon dioxide, and mounted on SEM specimen stubs. Samples were sputter-coated with a 10 nm layer of gold and evaluated in a JEOL JSM-840 SEM at 5–10 kV.

2.5. Transmission electron microscopy (TEM)

Erythrocytes were incubated with purified VHH (16 HU) for 5, 20, 45 min and 2 h, and then fixed in 2.5% glutaraldehyde for 4 h. Eight 25-cm^2 cell culture flasks were individually seeded with 1×10^5 FG-9307 cells into MEM with 10% BCS and incubated with VHH (16 HU). Cells incubated without VHH were taken as controls. After 2 days of culturing at 20 °C, the cells were re-suspended in the culture medium using a cell blade. Then, the cells were collected by centrifugation at 2000 *g* for 10 min and fixed using 2.5% glutaraldehyde for 4 h.

The samples were postfixed in 1% OsO_4 in 0.9% NaCl for 30 min, dehydrated in a graded series of acetone/water (50–100%, v/v) and finally embedded in Epon. Sections were cut in a Reichert-Jung ultramicrotome and collected on Formvar coated Ni or Cu grids (200 mesh). The sections were stained with lead acetate and post-stained with uranyl acetate before examination in a JEM-1200EX electron microscope (Jeol, Tokyo, Japan).

2.6. Immunogold localization of VHH on flounder cells treated with VHH

Ultrasections of erythrocytes and FG-9307 cells were collected on Formvar coated Ni grids. Sections were blocked with TBS (pH 7.2) containing 0.1% bovine serum albumin and incubated overnight in a drop of rabbit anti-VHH polyclonal antibody (1:100 in TBS, pH 7.2) [4]. This was followed by three drop washes of TBS (pH 7.2) and TBS (pH 8.2), respectively, and sections were then incubated for 60 min with goat anti-rabbit colloidal gold conjugates (particle size, 10 nm, Sigma–Aldrich) (1:50 in TBS, pH 8.2). Sections were then washed in TBS (pH 8.2), TBS (pH 7.2) and distilled water, air-dried and counterstained with uranyl acetate. Electron micrographs were obtained using a JEM-1200EX electron microscope.

2.7. DAPI staining

FG-9307 cells were seeded onto chamber slides at a density of 1×10^5 cells per well, incubated at 20 °C for 24 h, and exposed to VHH (2.5 μg/ml) for 24 h. The cells were fixed with 4% paraformaldehyde at 4 °C for 25 min, and then permeabilized with 0.1% Triton X-100. After washing twice with PBS (pH 7.4), slides were DAPI (0.5 μg/ml, Roche, Germany) stained and observed under a fluorescence microscope (Nikon, Eclipase E600, Tokyo, Japan).

2.8. TUNEL assay

FG-9307 cells were grown on coverslips at a density of 1×10^5 cells per well in a 6-well plate and exposed to VHH for 24 h. Using a One Step TUNEL Apoptosis Assay Kit (Beyotime Biotech., Jiangsu, China), the cells were observed under fluorescence microscopy for apoptosis.

2.9. Flow cytometry analysis

FG-9307 cells were treated with VHH (2.5 μg/ml) for 24 h. All cells, both adherent and suspended, were collected, washed, and suspended in cold PBS (pH 7.4). The cells were fixed in chilled 75% methanol and stained with a propidium iodine (PI) solution (100 μg/ml RNase and 10 μg/ml PI in PBS). Data acquisition and analysis were carried out using Modifit and CellQuest Software with a flow cytometry system (Becton and Dickinson, USA).

2.10. Caspase-3 assay

Ten-ml cultures of FG-9307 cells at 1×10^5 cells/ml were incubated for 24 h with VHH (2.5 μg/ml). The caspase-3 activity was determined using colorimetric assay kits (Beyotime Biotech.) according to the instruction. Briefly, cells were collected and lysed using lysate buffer. After that, 40 μl of the cell lysate (cytosolic extracts, 100 μg) was mixed with 50 μl of reaction buffer and 10 μl of Ac-DEVD-pNA substrates, and incubated at 37 °C for 2 h. After incubation, the chromophores were quantified spectrophotometrically at a wavelength of 405 nm.

2.11. Statistical analysis

Data of caspase activities are expressed as means ± SD of at least three individual experiments and were compared using a paired *t*-test. Statistical significance was set at $p < 0.01$.

3. Results

3.1. Ultrastructural changes in flounder erythrocytes exposed to VHH

Representative micrographs showing structural changes in erythrocytes at different stages of lysis after exposure to VHH are shown in Fig. 1. Control cells had an oval shape, a smooth membrane contour and an intact interior structure (Fig. 1A and B). Echinocytic shaped cells with thin tubular protrusions were observed after erythrocytes were treated with VHH for 5 min; and

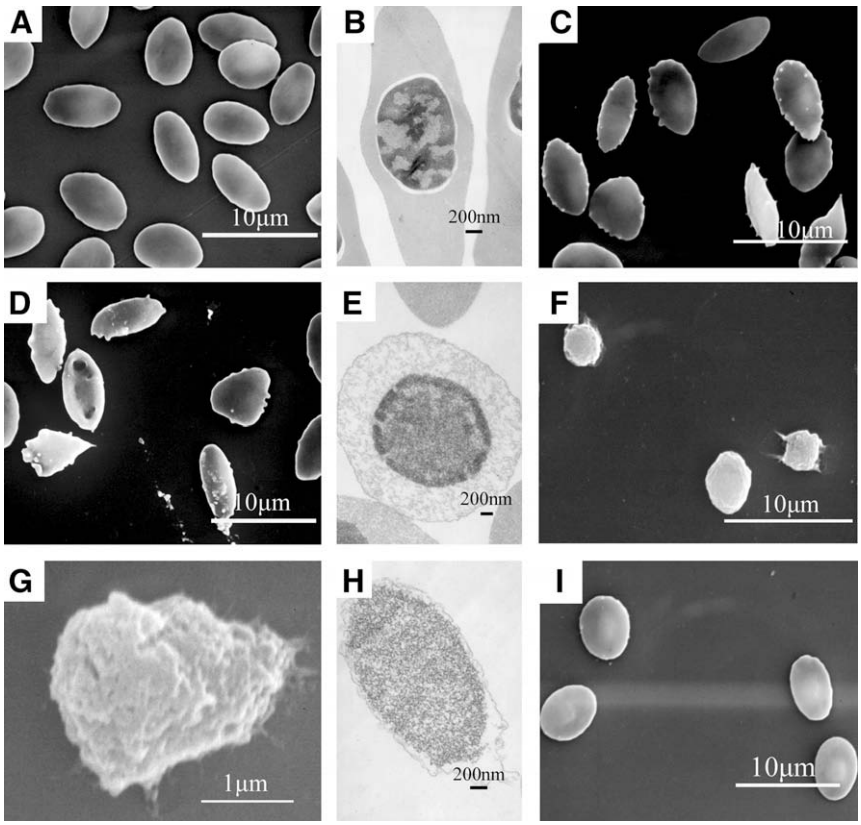

Fig. 1. Ultrastructural changes in flounder erythrocytes induced by VHH. A, C, D, F, G and I were observed under SEM; B, E and H were observed under TEM. Untreated cells (A, B); cells treated with 16 HU of VHH for 20 min (C), 45 min (D, E) and 2 h (F–H); cells treated with mutant VHH for 2 h (I).

no obvious changes could be observed in the interior of the erythrocytes. After 20 min incubation, bouquets of tubular protrusions from the plasma membrane developed, culminating in the occurrence of echinocytic spicula around the cell rim (Fig. 1C). The protrusions on the surface of erythrocytes rapidly increased in number with extended incubation times. Incubation of erythrocytes with VHH for 45 min resulted in membrane lesions; damage was to the extent that some erythrocytes formed huge holes (Fig. 1D). In the interior of the cells, great changes occurred both in the cytoplasmic and nuclear areas. Degeneration of the cytoplasm and disintegration of the nucleus was observed; the chromatin of the nucleus became homogeneous, and erythrocytic hemoglobin was released into the extracellular space (Fig. 1E). When the incubation time reached 2 h, some erythrocytes were completely destroyed (Fig. 1F) and membrane corrugations were clearly observed at high magnification (Fig. 1G). Overall, the contour of the membrane became irregular, almost all of the hemoglobin was released into the extracellular environment, fragments of the chromatin were dispersed throughout the cell, and the cells were permeated with debris (Fig. 1H). In contrast, mutant VHH did not perturb the overall erythrocyte shape, with the exception of a slight cell sphering being induced after incubation for 2 h (Fig. 1I). However, no well-defined 'echinocytic' shapes with large broad spicula were observed in erythrocytes following incubation with the mutant protein. Also, the interior structure of the erythrocyte was as complete as the control cell even after 2 h treatment with mutant VHH (data not shown).

3.2. Ultrastructural changes of FG-9307 cells exposed to VHH

The control FG-9307 cells bore conspicuous nuclei, lysosomes and Golgi apparatus, a large number of mitochondria and numerous cisternae of endoplasmic reticulum (ER) at the periphery of the nuclei (Fig. 2A and B). In contrast, after incubation with VHH for 48 h, the fine structure of the cell was destroyed, few organelles remained visible, and the chromatin was condensed significantly, forming a high-density area. Many particles with smooth contours formed within the cell, and some of these particles were electron dense, features resembling apoptotic bodies (Fig. 2C). In other cells, the chromatin was less condensed, and the membrane of the cell degraded, which caused the release of many particles as well (Fig. 2D).

3.3. Localization of VHH in flounder cells treated with VHH

The presence of VHH was visualized as electron dense gold particles of 10 nm. For erythrocytes at the early stage of reaction with VHH (after 20 min incubation), immunoreactions were observed in the cytoplasm, nucleus and cell membrane; after longer incubation times of up to 2 h, the cells were nearly destroyed, and numerous immunoreactive VHH particles were visualized throughout the cytoplasmic membrane (Fig. 3A). In contrast, only a few gold particles localized to the cytoplasm of those erythrocytes challenged by the mutant VHH. For the FG-9307 cells, a few colloidal gold particles were noticed on the membrane of the cells (Fig. 3B). No obvious labeling of VHH was shown on the control cells of both erythrocytes and FG-9307 cells (Fig. 3).

3.4. Apoptotic bodies and TUNEL positive cells induced by VHH in FG-9307 cells

To confirm the existence of apoptosis, the morphological changes of VHH-treated FG-9307 cells were followed. Using DAPI staining, cell shrinkage, chromatin condensation (Fig. 4A upper right) and typical apoptotic bodies (Fig. 4A upper right insert) were observed in FG-9307 cells exposed to VHH. In addition, results of

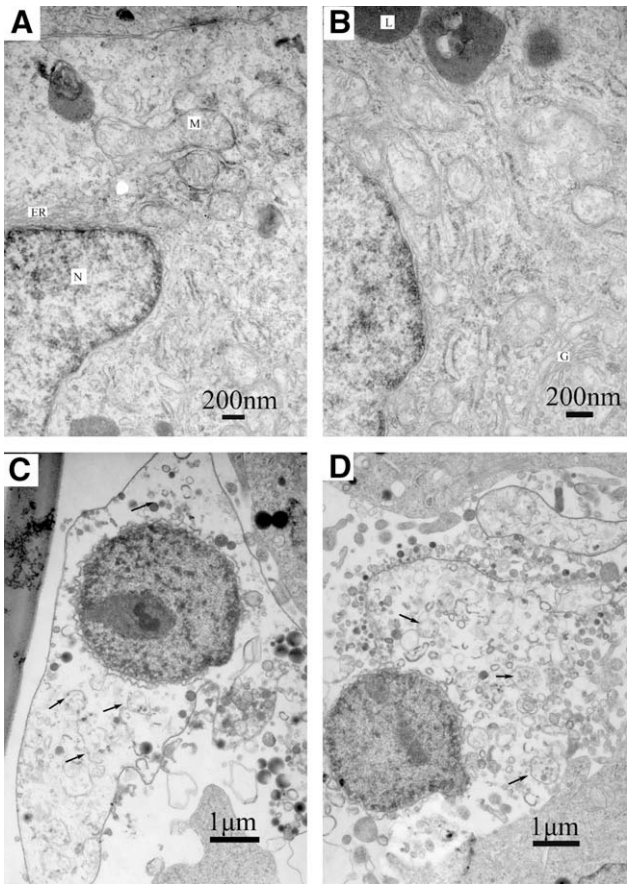

Fig. 2. Ultrastructural changes in flounder FG-9307 cells induced by VHH. Shown are ultrathin sections of control cells (A, B) and cells after treatment with VHH (C, D) by TEM. (A) Nucleus, endoplasmic reticulum and mitochondria; (B) Lysosomes and Golgi apparatus; (C, D) Few visible organelles were noted and some potential apoptotic bodies (arrows) formed. N, nucleus; ER, endoplasmic reticulum; M, mitochondrion; L, lysosome; G, Golgi apparatus.

TUNEL assay showed that VHH significantly increased the number of TUNEL positive cells (Fig. 4A lower right). In contrast, unexposed cells had a normal healthy appearance and did not show signs of chromatin condensation, apoptotic bodies (Fig. 4A upper left) and TUNEL positive cells (Fig. 4A lower left).

3.5. Increased apoptotic percentage induced by VHH in FG-9307 cells

As shown in Fig. 4B, FG-9307 cells cultured in the presence of VHH had ~99.8% of cells in the G1 phase compared with only 60.8% in the untreated control cells. VHH significantly increased apoptosis percentage to ~51.5% in FG-9307 cells 24 h after VHH treatment compared with only 0.1% in the untreated cells, suggesting that VHH can induce apoptosis, but not necrosis.

3.6. Activation of caspase-3 by VHH in FG-9307 cells

Caspase-3 is a key mediator of apoptosis. To evaluate the possible involvement of downstream effector caspases, the activity of caspase-3 was monitored in FG-9307 cells following VHH treatment. Compared to untreated controls, incubation of FG-9307 cells with VHH resulted in a 2.3-fold increase in caspase-3 activity (Fig. 4C).

4. Discussion

In this study, the cytotoxicity of VHH to both flounder erythrocytes and gill cells were studied, and it was found that the erythrocytes were much more sensitive to VHH than the gill cells. About 50% of the erythrocytes (10^6 cells/ml) were stained by trypan blue when it was treated with VHH (2.5 μg/ml) for 8 h, while only 1% of the FG-9307 cells died under the same condition (data not shown).

We found that VHH-induced tubular protrusions of erythrocyte membrane after short-time incubation. Similar tubular protrusions were also induced by amphiphile in rainbow trout (*Onchorhynchus mykiss*) erythrocytes [17]. VHH, or the catalyzed products of VHH, might have an amphiphile-like structure and might affect erythrocytes in a similar fashion. Also, we have demonstrated that active-site mutant VHH, which could disrupt hemolytic and phospholipase activities [15], induced slight protrusions in flounder erythrocyte membrane. This suggested that the protein-based induction of protrusions might also depend on other domains of the protein, in addition to the active-site that interacts with VHH.

In a previous study, we demonstrated that VHH has phospholipase activity [4]. In this study, both exterior and interior structures of flounder erythrocytes were completely destroyed by VHH. In contrast, the active-site mutant VHH, which has lost phospholipase activity, induced no obvious changes in the erythrocytes. This finding indicated that the phospholipase activity of VHH plays a major role in hemolysis. Since phospholipids are the major component of cell membranes, shape transformations caused by VHH are thought to mainly depend on the disruption of that major component, the phospholipids.

Previously, we reported that VHH was cytotoxic to FG-9307 cells in tissue culture [4]. In this study, the effect of VHH on FG-9307 cells was studied at the ultrastructural level. The definite structure of FG-9307 cells was destroyed, almost to the point that no visible organelles were evident after treatment with VHH. Similarly, Li and Zhang [18] reported only a few visible organelles remained in FG-9307 cells after exposure to the organophosphorus pesticide, parathion. On the contrary, in human amniotic membrane cells (FL cells), TDH of *V. parahaemolyticus* caused disappearance of microvilli from cell surface, degeneration of cytoplasm, and nuclear disintegration [19].

Localization of VHH to erythrocytes and FG-9307 cells, via immunogold staining technique after incubation with VHH, illustrated numerous gold particles were mainly deposited on the cytoplasmic membrane of erythrocytes and FG-9307 cells. However, a few gold particles were also deposited on the interior structure of these cells. This observation suggested that the cytoplasmic membrane of erythrocyte is not the sole target of VHH. We previous demonstrated that VHH is a lysophospholipase or a phospholipase B, which belongs to the GDSL enzyme family [15]. GDSL hydrolases have a flexible active-site that appears to change conformation and thereby exhibit binding to a variety of substrates. Some of the GDSL enzymes have thioesterase, protease, arylesterase, and lysophospholipase activities [20]. VHH might also have a flexible active-site capable of binding to a selection of substrates. In other words, VHH may have enzymatic activities other than phospholipase activity. Hence, it is understandable that VHH did not specifically act only on the cytoplasmic membrane of erythrocyte. A few gold particles were also present on the cytoplasm after incubation with mutant VHH, indicating that the mutant VHH retains the ability to bind to the erythrocyte. Similarly, a mutant toxin of TDH, which has a single amino acid substitution of serine for glycine 62, has been reported to have low hemolytic activity, but still remain approximately 50% of the binding ability of wild-type TDH [21].

Two mechanisms of eukaryotic cell death have thus far been identified: necrosis and apoptosis. In necrosis, the plasma membrane loses its ability to regulate osmotic pressure, and the cell swells and ruptures. The major morphological changes of apoptotic cell death are cell shrinkage, condensation of the nuclear chromatin, and fragmentation of the chromosomal DNA into multimers of

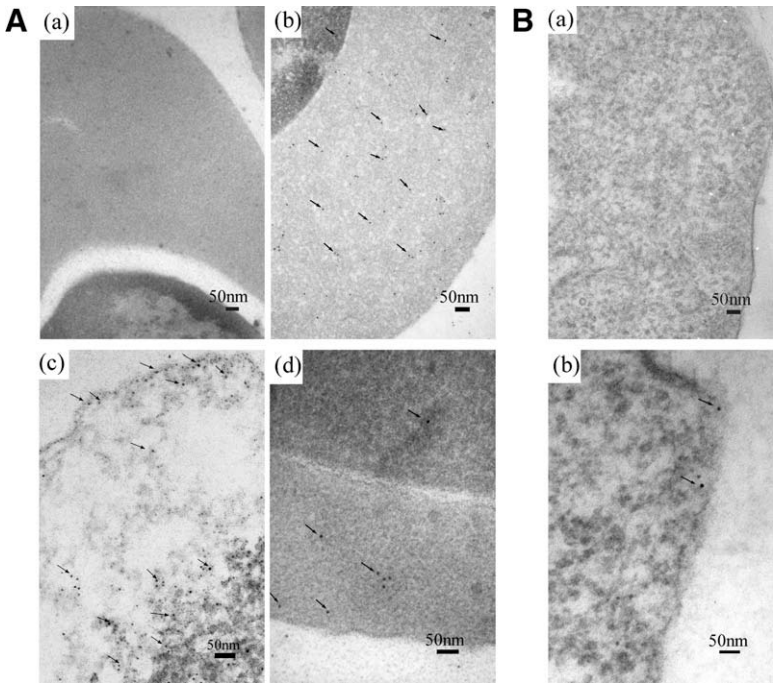

Fig. 3. Immunogold localization of VHH on erythrocytes and FG-9307 cells of flounder treated with VHH. Shown as immunogold particles of 10 nm (arrows). (A) Erythrocytes. Control cells (a) and cells incubated either with VHH for 20 min (b) and 2 h (c), or mutant VHH for 2 h (d); (B) FG-9307 cells. Showing control cells (a), and cytoplasmic membrane of cells (b) with VHH-treated for 48 h.

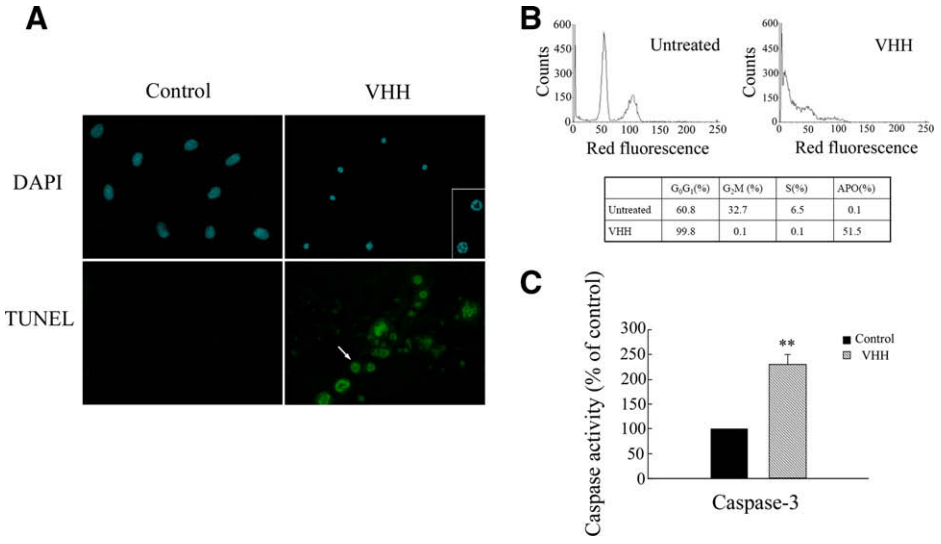

	G_0G_1(%)	G_2M (%)	S(%)	APO(%)
Untreated	60.8	32.7	6.5	0.1
VHH	99.8	0.1	0.1	51.5

Fig. 4. Apoptosis analysis of VHH-treated FG-9307 cells. (A) DAPI staining and TUNEL assay for apoptotic cells. The results are shown as a fluorescence microscopy image (400× magnification for DAPI staining and 1000× magnification for insert DAPI staining and TUNEL assay). Typical apoptotic bodies (upper right insert) and TUNEL positive cells (arrow) were formed in VHH-treated cells. (B) Cell cycle analysis. Cell cycle analysis was carried out using Modifit and CellQuest Software with flow cytometry. The table shows the percentages of cells in different phases of the cell cycle and apoptosis percentages in untreated and VHH-treated cells. (C) Caspase-3 activities. Data are reported as means ± SD from three independent experiments. $^{**}p < 0.01$ compared to untreated control.

200 bp [22]. In this study, apoptotic features such as chromatin condensation and apoptotic bodies were observed in VHH-treated FG-9307 cells. Also, VHH significantly increased apoptosis percentage and the number of TUNEL positive apoptotic cells. These findings strongly indicate that VHH kills the cells by inducing apoptosis rather than necrosis. However, a "secondary necrosis" (post-apoptotic) lead to cytoplasmic leakage at 48 h, a time-point at which the nucleus is still clearly showing apoptotic features. Similarly, apoptotic cell deaths were induced by the TDH of *V. parahaemolyticus* and Sph2, a sphigomyelinase hemolysin from *Leptospira interrogans* [23,24]. Furthermore, Masamune et al. [12] reported that lysophosphatidylcholine (lyso-PC), phospholipase A2-generated phospholipid by-products, induced apoptosis in rat pancreatic AR42J cells. We hypothesize that VHH triggers apoptosis in FG-9307 cells by lyso-PC, the catalyzed products of VHH, in the same manner.

Caspase, a family of cysteine proteases, plays a major role in the intracellular signal pathway in apoptosis. The caspases generally consist of the upstream initiator caspases such as caspase-2, -8, -9 and -10, and the downstream effector caspases such as caspase-3,

-6 and -7 [25]. Caspases cascade can be triggered by activation of the cell surface receptor or by mitochondria, and the activated caspases can cleave various substrates and cause typical apoptotic changes to the cells and nuclei [26]. In many animal cells, the execution phase of apoptosis correlates with the activation of caspase-3 [27,28]. In this study, it was found that caspase-3 was activated by VHH, implying that the caspase activation pathway is involved in VHH-induced apoptosis. Similarly, Shiga toxin from enterohemorrhagic *Escherichia coli* can activate caspase-3 and induce apoptosis in THP-1 human monocytic cells [29]. However, the TDH of *V. parahaemolyticus* induces apoptosis in Rat-1 cells in a caspase-independent manner, due to the broad-spectrum caspase initiator being unable to inhibit apoptosis [23].

In conclusion, the results obtained in this study demonstrate that the action of VHH mainly depends on the disruption of the phospholipids component of cellular membrane. Additionally, VHH can induce apoptosis in FG-9307 cells via the caspase activation pathway. These findings provide new insights into the VHH-mediated pathogenicity mechanism of *V. harveyi* to eukaryotic cells.

Acknowledgments

This work was supported by grants from the National Natural Science Foundation of China (No. 30771656), NSFC-RGC Joint Research Scheme (30831160512 from NSFC, China, and N_CUHK447/08 from RGC, Hong Kong), a key project of Chinese Ministry of Education (No. 108082), and the Key Laboratory of Experimental Marine Biology, Institute of Oceanology, Chinese Academy of Sciences.

References

[1] B. Austin, X.H. Zhang, *Vibrio harveyi*: a significant pathogen of marine vertebrates and invertebrates, Lett. Appl. Microbiol. 43 (2006) 119–124.
[2] S. Wilkins, M. Millar, S. Hemsworth, G. Johnson, S. Warwick, B. Pizer, *Vibrio harveyi* sepsis in a child with cancer, Pediatr. Blood Cancer 50 (2007) 891–892.
[3] X.H. Zhang, B. Austin, Pathogenicity of *Vibrio harveyi* to salmonids, J. Fish Dis. 23 (2000) 93–102.
[4] Y. Zhong, X.H. Zhang, J. Chen, Z. Chi, B. Sun, Y. Li, B. Austin, Overexpression, purification, characterization and pathogenicity of *Vibrio harveyi* haemolysin VHH, Infect. Immun. 74 (2006) 6001–6005.
[5] X.H. Zhang, B. Austin, Haemolysins in *Vibrio* species, J. Appl. Microbiol. 98 (2005) 1011–1019.
[6] G.E. Rowe, R.A. Welch, Assays of haemolytic toxins, Methods Enzymol. 235 (1994) 657–669.
[7] S. Pal, A. Datta, G.B. Nair, B. Guhathakurta, Use of monoclonal antibodies to identify phospholipase C as the enterotoxic factor of the bifunctional hemolysin-phospholipase C molecule of *Vibrio cholerae* O139, Infect. Immun. 66 (1998) 3974–3977.
[8] M.W. Parker, S.C. Feil, Pore-forming protein toxins: from structure to function, Prog. Mol. Biol. Biophys. 88 (2005) 91–142.
[9] D.E. Niewoehner, K. Rice, A.A. Sinha, D. Wangensteen, Injurious effects of lysophosphatidylcholine on barrier properties of alveolar epithelium, J. Appl. Physiol. 63 (1987) 1979–1986.
[10] H.U. Weltzien, Cytolytic and membrane-perturbing properties of lysophosphatidylcholine, Biochim. Biophys. Acta 559 (1979) 259–287.
[11] N. Kume, M.I. Cybulsky, M.A. Gimbrone Jr., Lysophosphatidylcholine, a component of atherogenic lipoproteins, induces mononuclear leukocyte adhesion molecules in cultured human and rabbit arterial endothelial cells, J. Clin. Invest. 90 (1992) 1138–1144.
[12] A. Masamune, Y. Sakai, A. Satoh, M. Fujita, M. Yoshida, T. Shimosegawa, Lysophosphatidylcholine induces apoptosis in AR42J cells, Pancreas 22 (2001) 75–83.
[13] X.H. Zhang, P.G. Meaden, B. Austin, Duplication of hemolysin genes in a virulent isolate of *Vibrio harveyi*, Appl. Environ. Microbiol. 67 (2001) 3161–3167.
[14] M. Nishibuchi, J.B. Kaper, Nucleotide sequence of the thermostable direct hemolysin gene of *Vibrio parahaemolyticus*, J. Bacteriol. 162 (1985) 558–564.
[15] B. Sun, X.H. Zhang, X. Tang, S. Wang, Y. Zhong, J. Chen, B. Austin, A particular single residue change in *Vibrio harveyi* hemolysin (VHH) results in the loss of phospholipase and hemolytic activities and pathogenicity to turbot (*Scophthalmus maximus*), J. Bacteriol. 189 (2007) 2575–2579.
[16] S.L. Tong, H. Li, H.Z. Miao, The establishment and partial characterization of a continuous fish cell line FG-9307 from the gill of flounder *Paralichthys olivaceus*, Aquaculture 156 (1997) 327–333.
[17] H. Hägerstrand, M. Danieluk, M. Bobrowska-Hägerstrand, A. Iglic, A. Wróbel, B. Isomaa, M. Nikinmmaa, Influence of band 3 protein absence and skeletal structures on amphiphile- and Ca^{2+}-induced shape alterations in erythrocytes: a study with lamprey (*Lampetra fluviatilis*), trout (*Onchorhynchus mykiss*) and human erythrocytes, Biochim. Biophys. Acta 1466 (2000) 125–138.
[18] H. Li, S. Zhang, In vitro cytotoxicity of the organophosphorus pesticide parathion to FG-9307 cells, Toxicol. In Vitro 15 (2001) 643–647.
[19] J. Sakurai, T. Honda, Y. Jinguji, M. Arita, T. Miwatani, Cytotoxic effect of the thermostable direct hemolysin produced by *Vibrio parahaemolyticus* on FL cells, Infect. Immun. 13 (1976) 876–883.
[20] C.C. Akoh, G.C. Lee, Y.C. Liaw, T.H. Huang, J.F. Shaw, GDSL family of serine esterases/lipases, Prog. Lipid. Res. 43 (2004) 534–552.
[21] G.Q. Tang, T. Iida, K. Yamamoto, T. Honda, A mutant toxin of *Vibrio parahaemolyticus* thermostable direct hemolysin which has lost hemolytic activity but retains ability to bind to erythrocytes, Infect. Immun. 62 (1994) 3299–3304.
[22] M.J. Arends, A.H. Wyllie, Apoptosis: mechanisms and roles in pathology, Int. Rev. Exp. Pathol. 32 (1991) 223–254.
[23] R. Naim, I. Yanagihara, T. Iida, T. Honda, *Vibrio parahaemolyticus* thermostable direct hemolysin can induce an apoptotic cell death in Rat-1 cells from inside and outside of the cells, FEMS Microbiol. Lett. 195 (2001) 237–244.
[24] Y. Zhang, Y. Geng, J. Yang, X. Guo, G. Zhao, Cytotoxic activity and probable apoptotic effect of Sph2, a sphigomyelinase hemolysin from *Leptospira interrogans* strain Lai, BMB Rep. 41 (2008) 119–125.
[25] Y. Shi, Mechanisms of caspase activation and inhibition during apoptosis, Mol. Cell 9 (2002) 459–470.
[26] S. Nagata, Apoptosis by death factor, Cell 88 (1997) 355–365.
[27] K. Kuida, T.S. Zheng, S. Na, C.Y. Kuan, D. Yang, H. Karasuyama, P. Rakic, R.A. Flavell, Decreased apoptosis in the brain and premature lethality in CPP32-deficient mice, Nature 384 (1996) 368–372.
[28] M. Miura, H. Zhu, R. Rotello, E.A. Hartwieg, J. Yuan, Induction of apoptosis in fibroblasts by IL-1β-converting enzyme, a mammalian homologue of the *C. elegans* cell death gene *ced-3*, Cell 75 (1993) 653–660.
[29] S. Kojio, H.M. Zhang, M. Ohmura, F. Gondaira, N. Kobayashi, T. Yamamoto, Caspase-3 activation and apoptosis induction coupled with the retrograde transport of Shiga toxin: inhibition by brefeldin A, FEMS Immunol. Med. Microbiol. 29 (2000) 275–281.